Available online at ScienceDirect

Nuclear Engineering and Technology

journal homepage: www.elsevier.com/locate/net

Original Article

Enhancement of Pool Boiling Heat Transfer in Water Using Sintered Copper Microporous Coatings

Seongchul Jun [a], *Jinsub Kim* [a], *Donggun Son* [b], *Hwan Yeol Kim* [b], *and Seung M. You* [a,*]

[a] *Department of Mechanical Engineering, The University of Texas at Dallas, 800 West Campbell Road, Richardson, TX 75080, USA*

[b] *Korea Atomic Energy Research Institute (KAERI), Severe Accident & PHWR Safety Division, 989-111 Daedeok-Daero, Yuseong-Gu, Daejeon, Korea*

ARTICLE INFO

Article history:
Received 24 November 2015
Received in revised form
3 February 2016
Accepted 23 February 2016
Available online 19 March 2016

Keywords:
Critical Heat Flux
Microporous Coating
Nucleate Boiling Heat Transfer
Pool Boiling
Sintering

ABSTRACT

Pool boiling heat transfer of water saturated at atmospheric pressure was investigated experimentally on Cu surfaces with high-temperature, thermally-conductive, microporous coatings (HTCMC). The coatings were created by sintering Cu powders on Cu surfaces in a nitrogen gas environment. A parametric study of the effects of particle size and coating thickness was conducted using three average particle sizes (APSs) of 10 μm, 25 μm, and 67 μm and various coating thicknesses. It was found that nucleate boiling heat transfer (NBHT) and critical heat flux (CHF) were enhanced significantly for sintered microporous coatings. This is believed to have resulted from the random porous structures that appear to include reentrant type cavities. The maximum NBHT coefficient was measured to be approximately 400 kW/m^{2}k with APS 67 μm and 296 μm coating thicknesses. This value is approximately eight times higher than that of a plain Cu surface. The maximum CHF observed was 2.1 MW/m^2 at APS 67 μm and 428 μm coating thicknesses, which is approximately double the CHF of a plain Cu surface. The enhancement of NBHT and CHF appeared to increase as the particle size increased in the tested range. However, two larger particle sizes (25 μm and 67 μm) showed a similar level of enhancement.

1. Introduction

There is worldwide concern regarding the safety of nuclear power plants as a result of the Fukushima Daiichi Nuclear Power Plant disaster. Systematic and robust accident management strategies are required to prevent a catastrophic failure even when a power plant is subject to abnormal conditions, such as a natural disaster. One of the major concerns

* *Corresponding author.*
E-mail address: you@utdallas.edu (S.M. You).
http://dx.doi.org/10.1016/j.net.2016.02.018

during such adverse conditions is the behavior of the molten corium, which can be produced during a severe accident when the core material inside the reactor is melted. This molten corium must be retained inside the reactor wall. If it penetrates the wall and flows out, it could cause a nuclear disaster such as that at Fukushima. There are two major mitigation measures: the first is to provide a corium catcher where the outflowing molten corium is gathered, the second is to develop more efficient and enhanced cooling solutions for the reactor wall. The second solution is desirable because it retains the corium inside the wall before the outflow. With current cooling technologies, the reactor wall is cooled by water, which boils due to the high heat flux from the molten corium. A key strategy considered herein is to improve the boiling heat transfer on the reactor wall using every technology possible.

In order to enhance either nucleate boiling heat transfer (NBHT) or critical heat flux (CHF) on a metal substrate, numerous surface treatments have been developed thus far. Among them, microporous coating is known to be one of the most effective surface treatments, owing to its micron-size pores including reentrant cavities. O'Connor and You [1] developed a novel painting technique to create microporous coatings consisting of 3-μm to 10-μm silver flakes on an aluminum foil using a thermal epoxy and a coating thicknesses of approximately 25 μm, and conducted a pool boiling experiment in a saturated FC-72 fluid. They reported that the CHF of the coated surface enhanced the boiling heat transfer by 400% and the CHF by 109%. O'Connor et al [2] further developed microporous coatings by spraying a coating using 0.3-μm to 3-μm aluminum particles at a thickness of approximately 10 μm, and painting 8-μm to 12-μm diamond particles at a thickness of 40 μm to 45 μm onto an aluminum foil. In addition, the authors conducted pool boiling on FC-72 and showed that CHF increased by 47% and 103%, respectively. Chang and You [3] created a microporous coating using Cu particles with an average size of 1 μm to 50 μm and a coating thickness of approximately 100 μm and using aluminum particles with an average size of 1 μm to 20 μm and a coating thickness of approximately 50 μm onto a plain Cu surface. The coatings were formed and bonded to the surface using an epoxy. They reported that the CHF was enhanced by approximately 100% and that the NBHT coefficient was enhanced by approximately 300% for both coatings in the pool boiling of FC-72 at 1 atm. Dizon et al [4] conducted a pool boiling experiment on water at 1 atm on an aluminum hemisphere shell surface with an outer diameter of 203 mm with spray-coated aluminum particles with particle sizes of 50 μm bonded by epoxy, and found that the CHF of the coated surface was 42% to 112% larger than the plain hemisphere aluminum surface, depending on the surface orientation. Li and Peterson [5] studied pool boiling enhancement of water using sintered Cu wire with diameters of 56 μm to 191 μm and of various thicknesses between 210 μm and 2,300 μm. They reported that the CHF increased with the coating thickness, up to 360 W/cm^2. However, they did not show boiling curves, nor NBHT coefficients. Kim et al [6] compared two different kinds of microporous coatings for R-123 and water at 1 atm. The first coating used aluminum powder on a Cu substrate and was bonded by epoxy, and various particle sizes were tested. They found that particle sizes of 8 μm to 12 μm maximized the enhancement of NBHT by approximately 270% and CHF by approximately 40% in R-123. The NBHT was enhanced the most by approximately 47% with particle sizes of 17 μm to 30 μm in water. The second coating used Cu powder with various particle sizes and was bonded by solder. They found that particle sizes of 53 μm to 88 μm and a coating thickness of approximately 175 μm enhanced the NBHT coefficient the most in water. The enhancement was approximately 460% and the CHF was enhanced by approximately 100%, compared to a plain Cu surface. Jun et al [7] created microporous coating by brazing 25-μm Cu particles on a Cu surface. They then studied the coating thickness effects on pool boiling enhancement at 1 atm in water. They reported that the maximum NBHT was found to be 350 kW/m^{2}K, which was approximately a 600% enhancement at a coating thickness of 96 μm, and that the maximum CHF was 2.1 MW/m^2 at a coating thickness of 225 μm, which was an approximate 100% enhancement compared to a plain Cu surface.

However, there have not been many results showing the effect of particle sizes and coating thicknesses on the NBHT and the CHF of microporous coatings, and the results that have been collected show certain conflicts. Lu and Chang [8] used sintered bronze particles of a 115 to 150 mesh and a coating thickness of double to 20 times the particle sizes, and concluded that the CHF was enhanced the most at a coating thickness of double the particle size and a 50% CHF enhancement in methanol, and that the CHF decreases as the coating thickness increases. Chang and You [9] reported on the effect of particle size on the CHF with 2 μm to 70 μm coated diamond particles bonded by epoxy, and showed in FC-72 that the CHF increases as the particle size increases. Hwang and Kaviany [10] used Cu brazed coatings with a particle size of 40 μm to 200 μm with a coating thickness of three to five times the particle size, and reported that the CHF showed an approximate 80% enhancement in n-pantane for all coatings, and that particle size has no significant effect on the CHF.

The purpose of the current work is to parametrically identify the effect of particle sizes and coating thicknesses of microporous coating created by sintering on the NBHT and the CHF in water at 1 atm. For this purpose, three different particle sizes, 10 μm, 25 μm, and 67 μm, with various coating thicknesses were tested.

2. Materials and methods

2.1. Test setup

A pool boiling chamber made of aluminum was used for the current pool boiling experimental study, as shown in Fig 1. Two tempered sight glasses were installed at the front and back for visualization. In order to heat and degas the working fluid, two immersion heaters were inserted in the chamber, and, to maintain the bulk fluid at a steady saturation temperature, two silicon band heaters were attached to two sides. Two T-type thermocouples were inserted through the top plate to measure the liquid and vapor temperatures, and a pressure transducer (0–138 kPa) was installed inside the chamber to measure the chamber pressure. An external, water-cooled condenser was connected to condense and

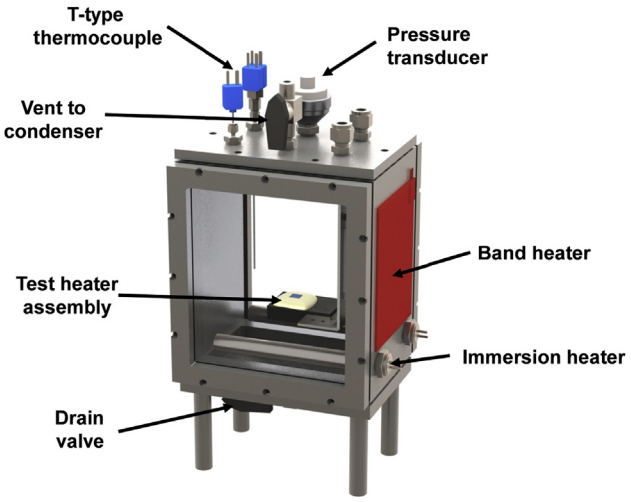

Fig. 1 – Schematic of the pool boiling chamber.

return the vapor generated, in order to maintain a constant liquid level in the chamber during the degassing and boiling tests. The test heater assembly was mounted on an aluminum bracket in the chamber. To drain the fluid, a drain valve was installed at the bottom of the chamber.

2.2. *Test heater*

The test heater assembly was fabricated as shown in Fig. 2. A Cu block (10 mm × 10 mm × 3 mm, $k = 401$ W/mK) was soldered to a resistive heater. A T-type thermocouple wire was inserted in the center of the Cu block to a depth of 5 mm from the side, and two electrical wires were soldered at each side of the bus bar. The Cu block/resistive heater pair was bonded to a Lexan substrate ($k = 0.2$ W/mK) using a 3M epoxy ($k = 0.18$ W/mK). The surface temperature was calculated from the temperature measured by the thermocouple assuming a one-dimensional vertical upper direction heat conduction through the Cu block. 3M epoxy was poured and cured around the Cu block and the resistive heater pair to provide insulation from the sides, as depicted in Fig. 2. The epoxy level was kept even with the test surface. The heat losses through the sides and bottom were negligible because the thermal conductivities of epoxy and Lexan were less than 1/2,000 compared to the Cu block.

2.3. *Test procedures*

The test chamber was heated to the saturation temperature at atmospheric pressure of distilled water, using the band and immersion heaters. The water was boiled vigorously for at least 45 minutes to remove dissolved noncondensable gases after the water reached the saturation temperature. A temperature controller connected to the band heaters ensured that the water was maintained at the saturation temperature at all times.

All pool boiling experiments in the current study were performed using the test heater assembly in the horizontal, upward facing orientation under increasing heat flux conditions until the CHF condition was reached. All boiling tests were repeated three times to ensure the consistency and repeatability of the data. A DC power supply (N5771A; Agilent Technologies, Santa Clara, CA, USA) and data acquisition system (34980A Multifunction Switch/Measure Unit; Agilent Technologies) were controlled using a LabVIEW program installed on a PC. An average of 40 test sample temperature measurements were taken over 20 seconds, and compared to the averaged value of the next 20 seconds after each heat flux increment. If the temperature difference between two consecutive averages was less than 0.1 K, a steady state was assumed and the temperature and applied heat flux values were recorded. Each instantaneous temperature measurement was compared to the previous averaged value, and when the difference exceeded 20 K, the DC power supply was shut down by the program and the CHF was assumed. The previous steady-state heat flux plus half of the heat flux increment was taken as the CHF value.

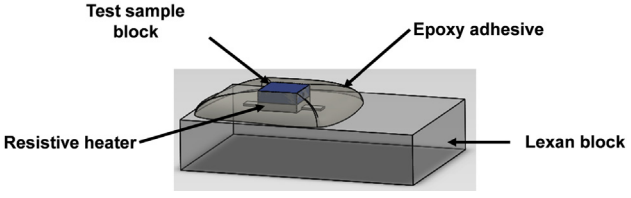

Fig. 2 – Schematic of test heater assembly.

2.4. *Microporous coatings fabrication*

The microporous coating was created by sintering a Cu powder on a Cu substrate. The mixture of the powder and thinner was poured and spread evenly on the Cu test surface. Then, the mixture was sintered and cooled in a furnace filled with nitrogen. The sintered Cu sample was cleaned in 5% acetic acid followed by acetone in an ultrasonic bath and finally rinsed with distilled water. The average particle sizes of the powder were measured by image processing of optical microscope images of Cu powders. The average sizes were 10 ± 1.4, 25 ± 9.0, and 67 ± 15 μm, as shown by the particle size distribution in Fig. 3. The coating thickness of each sample was measured using a micrometer. The coating is called High temperature, Thermally Conductive, Microporous Coating (HTCMC).

The HTCMC shows porous structures (Fig. 4). The coating is believed to have reentrant type cavities, which are stable in creating nucleating bubbles and has larger pores with larger particle sizes. The porosity (ε) of the HTCMC was obtained using the measured volume of porous layer (V_t) and the weight of Cu powders (m_{cp}):

$$\varepsilon = \frac{v_t - \left(m_{cp}/\rho_{cp}\right)}{V_t} \quad (1)$$

where ρ_{cp} is the density of Cu powders (= 8.96 g/cm^3). (See Table 1 for a list of nomenclature used.) The average porosities obtained were 0.52, 0.63, and 0.66 for APS 10 μm, 25 μm, and 67 μm, respectively. Fig. 5 shows that the porosity is independent of the coating thickness.

To characterize the wetting behavior of the HTCMC, the apparent contact angles were measured by dripping a single water drop of 11.5 μL (2.8 mm diameter) from a needle onto a HTCMC surface by using a goniometer (DSA30; Króss,

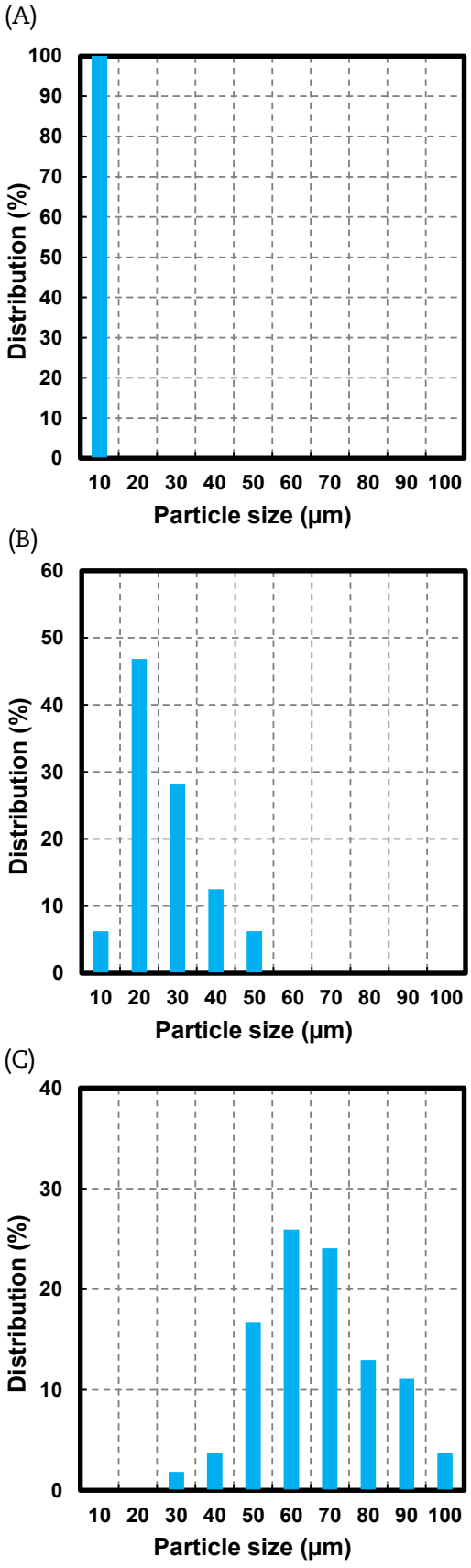

Fig. 3 – Particle size distribution. (A) Average particle size (APS) 10 μm, (B) APS 25 μm, and (C) APS 67 μm. The sizes were measured using an image processing program of optical microscope images of Cu powders.

Hamburg, Germany). The contact angle appeared to show a trend of reduction with the coating thickness and particle sizes as shown in Fig. 6. The contact angle decreased with thicker coating and larger particles due to effective wicking through the porous layer.

2.5. *Uncertainty analysis*

The experimental uncertainties for this study were estimated using the Kline and McClintock method [11]. Heat flux measurement uncertainty caused by the voltage, current, surface area of the heater, and heat losses through the epoxy and Lexan substrate was estimated to be less than 5% with a 95% confidence level. The uncertainty for the temperature measurement was estimated to be ± 0.5 K.

3. Results and discussion

The experimental study of pool boiling with Cu HTCMC surfaces created by sintering on a Cu block was conducted in distilled water at 1 atm to investigate the effect of particle size and coating thickness on the NBHT and CHF. Three APS of 10 μm, 25 μm, and 67 μm with various coating thicknesses were tested. For each particle size, the coating thickness was varied to find the most enhanced NBHT and CHF. The highest heat flux data point in each curve of the following figures indicates the last experimental data in the nucleate boiling regime, which are defined to be CHF.

At very thin coating thicknesses of less than 78 μm, 94 μm, and 296 μm for APS 10 μm, 25 μm, and 67 μm, respectively, both the NBHT and CHF enhancements gradually grow from those of a plain curve as the coating thickness increases. This behavior is illustrated in Fig. 7 for the 25-μm case. This is because the number of active nucleation sites increased owing to the porous structure and also because the boiling bubbles broke into smaller ones as they were nucleated and grew deep inside the cavities of the porous structure.

As discussed by Jun et al [7], the gradual enhancement of the NBHT coefficient of Cu HTCMC in Fig. 7 is attributed to its porous structure including many micron-scale cavities and larger embryonic bubbles formed at the reentrant-type cavities. The number of active nucleation sites is thus enormously increased, owing to the microporous structure compared to that of the plain Cu surface. This behavior is clearly shown later in Fig. 8.

Furthermore, the pores are interconnected as shown in Fig. 4. Therefore, bubbles growing at a nucleation site inside the microporous structure break into connected multiple pore openings through the layer and depart as numerous small bubbles. During this growth and departure process, cold bulk liquid is expected to be sucked into the other side pores. Numerous small bubble departures from the connected porous passage ways may cause oscillating capillary flows, which may further enhance the cooling efficiency.

Reentrant cavities are known to be very stable in the generation of nucleating bubbles due to the combination of cavity geometry and embryonic bubble radius along with thermodynamic aspects of the fluid. The effect of nucleating bubble

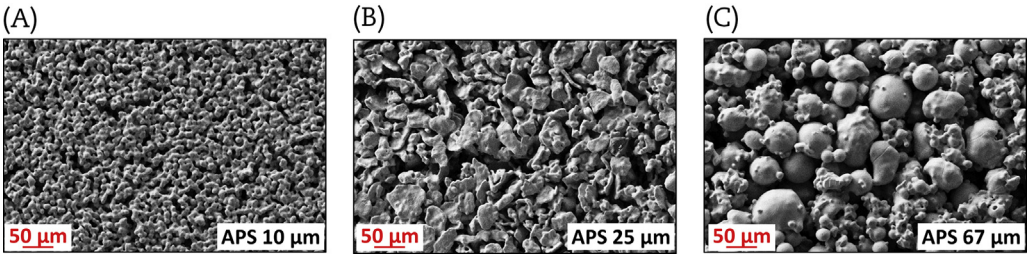

Fig. 4 – Scanning electron micrographs of sintered particles. (A) Average particle size (APS) 10 μm, (B) APS 25 μm, and (C) APS 67 μm.

radius on the wall superheat at saturation for a given system pressure can be modeled from the Young–Laplace and Clasius–Clapeyron equations [12]:

$$\Delta T_{sat} = \frac{2\sigma T_l V_{lv}}{L_{lv} R_c} \quad (2)$$

where R_c is the radius of liquid/vapor interface curvature in a cavity. With a larger R_c, a lower surface superheat (ΔT_{sat}) is required to make the bubble grow. The larger reentrant shape cavity will provide much larger R_c values in the HTCMC, compared to those of the plain Cu surface. With the many reentrant cavities distributed throughout the structure, the surface wall superheat required on the HTCMC surfaces has to be much lower, as shown in Fig. 7.

Images of the nucleate boiling heat transfer are shown in Fig. 8, all at one low heat flux (20 kW/m^2). The number of active nucleation sites are evidenced by the number of departing bubbles. It is much more in the porous coatings than that on a plain surface, as shown. Among the three porous coatings with different APS, the wall superheat values at the same low heat flux decrease as the particle size increases due to the larger pore sizes, as evidenced in the scanning electron microscope images of Fig. 4. The wall superheat was measured to be 7.8 K for plain Cu, 3.1 K for APS 10 μm, 2.1 K for APS 25 μm, and 1.4 K for APS 67 μm, all at 20 kW/m^2. Boiling initiates at a

Table 1 – Nomenclature.

Nomenclature	Description
h	Boiling heat transfer coefficient (W/m^{2}k)
k	Thermal conductivity (W/mk)
L	Latent heat (J/kg)
q″	Heat flux (W/m^2)
R	Radius (m)
T	Temperature (K)
ΔT_{sat}	Wall superheat (K)
v	Specific volume (m^3/kg)
Greek Symbols	
σ	Surface tension (N/m)
Subscripts	
c	Cavity
cp	Cu powder
l	Liquid
lv	Liquid–vapor
m	Microporous coating
p	Plain
sat	Saturated conditions

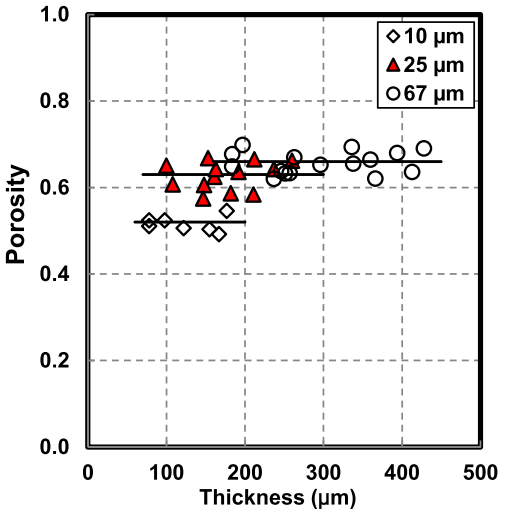

Fig. 5 – Porosity of average particle sizes 10 μm, 25 μm, and 67 μm with the coating thickness. The horizontal bars represent the average values of porosity of each particle size.

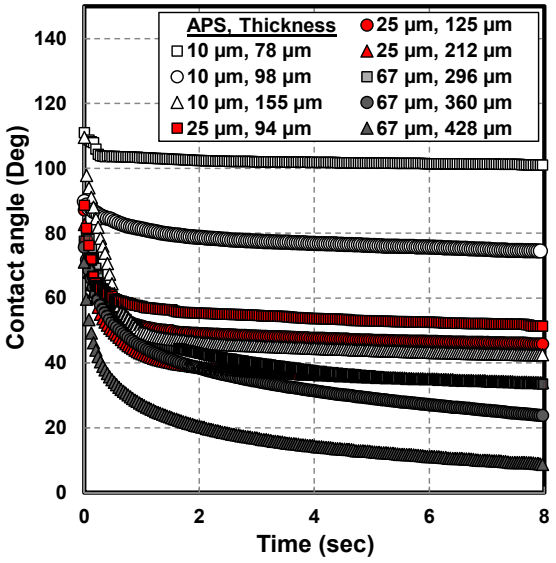

Fig. 6 – Apparent contact angles of average particle sizes 10 μm, 25 μm, and 67 μm with the coating thickness.

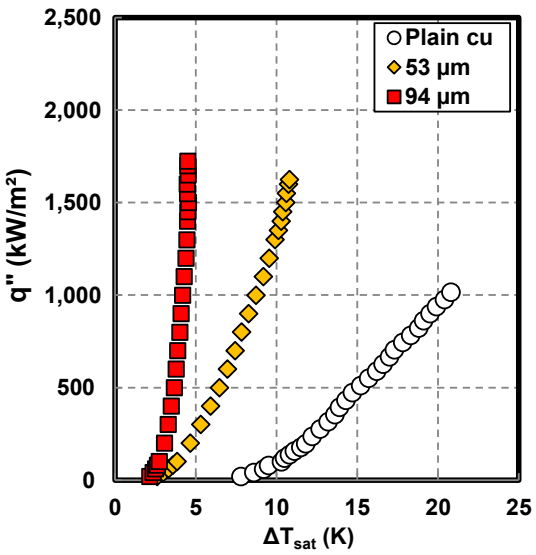

Fig. 7 – Boiling curves of plain and high-temperature, thermally-conductive, microporous coating (HTCMC) of average particle sizes 25 μm at very thin coating thickness region.

lower wall superheat with a larger pore size, and thus the number of activated nucleation sites appears to increase, as shown in the photographs in Fig. 8.

The boiling curves of different particle sizes are plotted with coating thickness variations in Fig. 9. The optimized coating thickness for NBHT, which has the smallest wall superheat prior to the CHF, was first found by increasing the coating thickness from a plain Cu surface, as shown for the 25-μm APS case in Fig. 7. For each particle size, the optimized thickness for NBHT is defined experimentally and plotted in the red square symbols in Fig. 9. For an APS of 10 μm, the optimized coating thickness was 78 μm, which is approximately eight times thicker than the particle size. For APS 25 and 67 μm, the coating thickness was 94 and 296 μm, respectively, and those are approximately four times the particle size [7,13]. The wall superheat in the nucleate boiling heat transfer regime near the CHF was approximately 6.5 K, 4.5 K, and 5.0 K for APS 10 μm, 25 μm, and 67 μm, respectively. As the coating thickness increased further from the optimized thicknesses, the NBHT coefficients generally decreased owing to the increasing thermal conduction resistance of the vapor inside the porous layer during boiling (Fig. 9). However, the NBHT performances of APS 25 μm and 67 μm showed slight enhancements at lower heat fluxes, but the thermal conduction resistances resulted in a decrease in NBHT as the heat flux

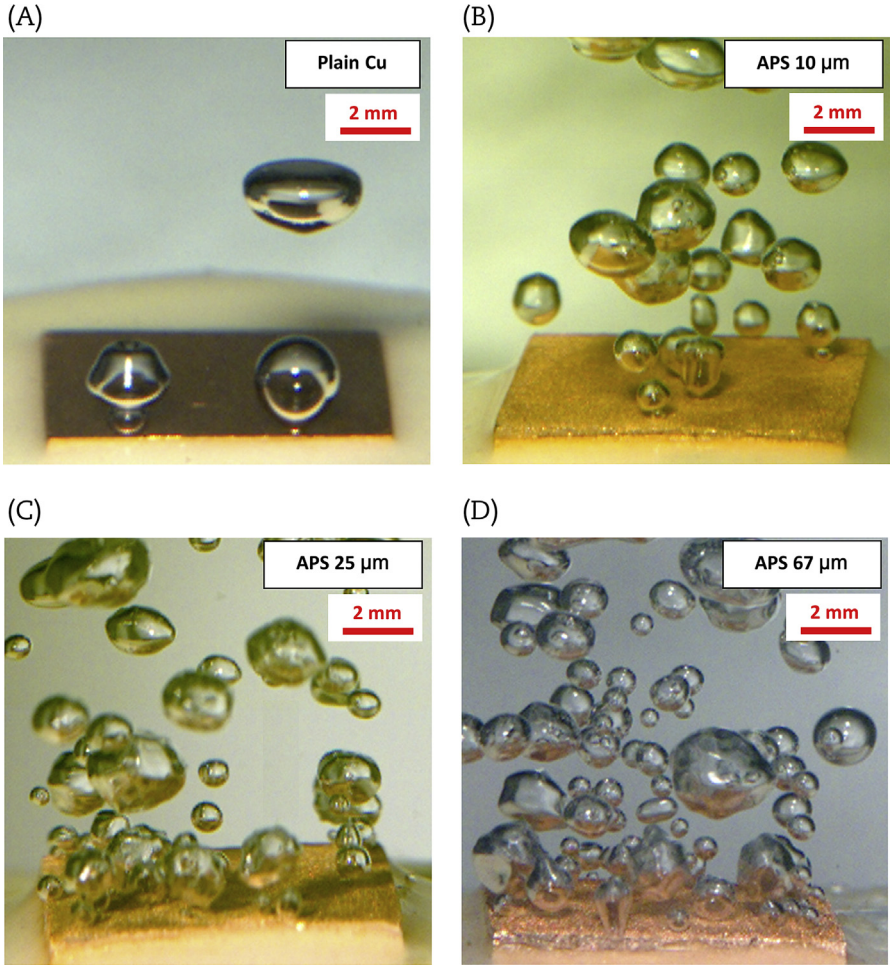

Fig. 8 – Nucleate boiling images at 20 kW/m². (A) Plain Cu, (B) average particle size (APS) 10 μm, (C) APS 25 μm, and (D) APS 67 μm Cu high temperature, thermally conductive, microporous coating (HTCMC).

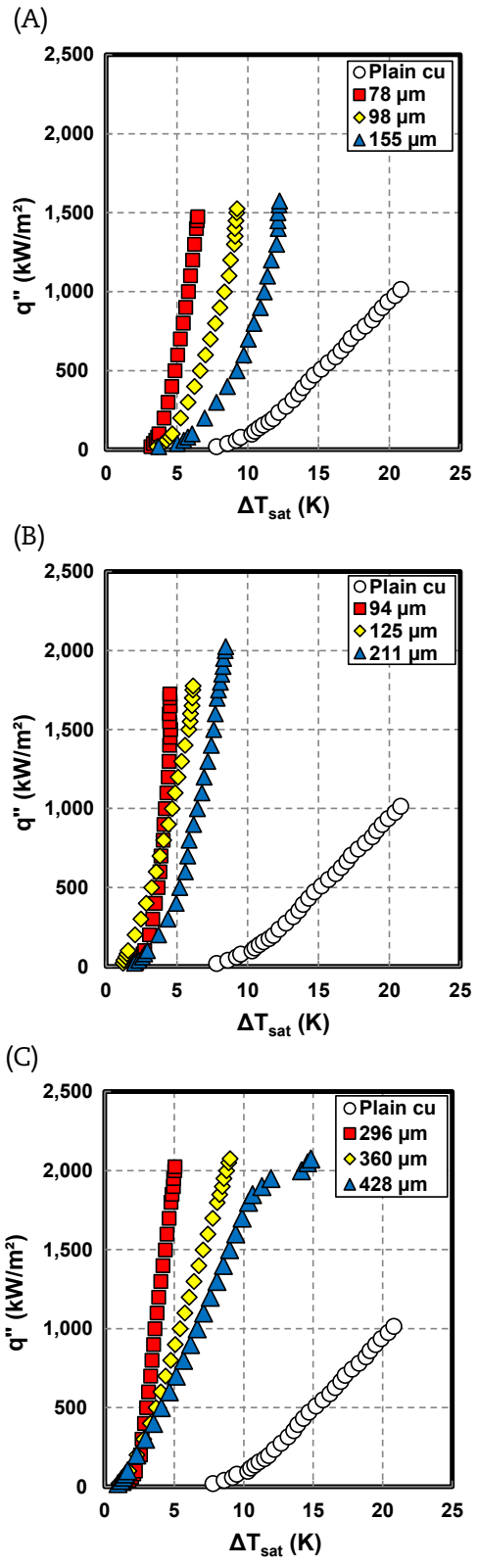

Fig. 9 – Pool boiling curves of water with a change of high temperature, thermally conductive, microporous coating thickness. (A) Average particle size (APS) 10 μm, (B) APS 25 μm, and (C) APS 67 μm.

increased further. Similar behavior was observed in the previous results of porous coatings [7,8,10]. To summarize, at very thin coatings below the optimized thickness, both NBHT and CHF enhancements gradually grow as the coating thickness increases. NBHT enhancement is due to the increase in active nucleation sites within the porous structure available to boil the liquid. Furthermore, CHF enhancement is because nucleated bubbles break into smaller ones, as bubbles are created and grow in the cavities inside of the porous layer. Both are discussed in details by Jun et al [7]. As coating thickness increases further than the optimized thickness, the thermal conduction resistance of the vapor in the porous layer tends to increase so the NBHT decreases while the CHF still continues to increase.

For APS 10 μm particle size, the CHF values are approximately 1,500 kW/m^2 or more, as shown in Fig. 10A. The maximum CHF for APS 10 μm was 1,575 kW/m^2 at a coating thickness of 155 μm. This value is an approximate 60% enhancement compared to that of the plain Cu surface case. It is noted in the figure that the CHF increased further from

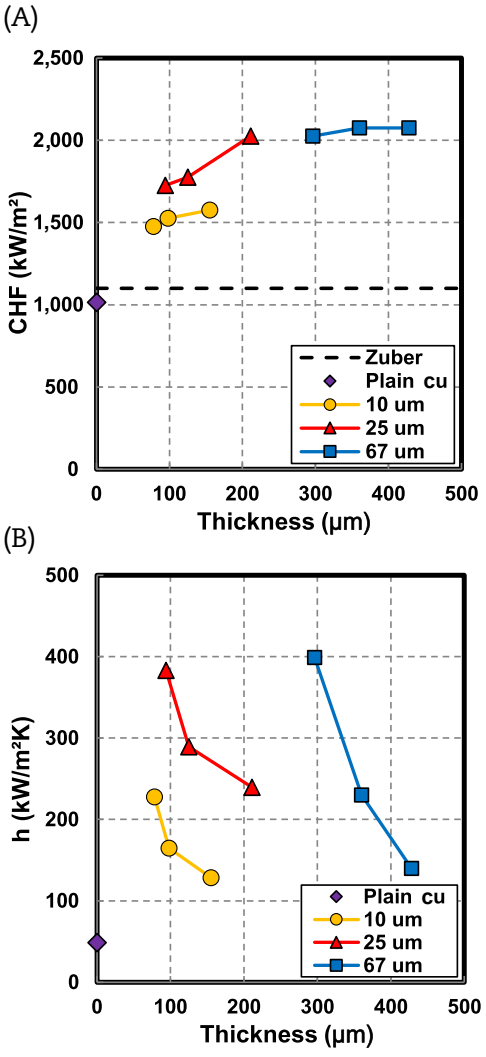

Fig. 10 – (A) Critical heat flux (CHF) with coating thickness and (B) Maximum nucleate boiling heat transfer coefficient with coating thickness.

approximately 1,500 kW/m^2 as the coating thickness increased for a 25 μm particle size of the APS. For the largest particle size of APS 67 μm, the CHF was consistently approximately 2,100 kW/m^2 for the range of the tested thicknesses in Fig. 10A. For the 25-μm and 67-μm APS cases, the maximum CHF enhancements showed an approximate 100% enhancement compared to that of plain Cu.

The maximum NBHT coefficients were calculated for different coating thicknesses with the three particle sizes from the data shown in Fig. 9 and plotted in Fig. 10B. They illustrated a trend of decreasing nucleate boiling heat transfer for increasing the thickness for all three particle sizes. The maximum h value, occurring at the optimized coating thickness for each particle size, increased as the particle size increased. The values obtained are 227 kW/m^{2}K, 383 kW/m^{2}K, and 399 kW/m^{2}K for 10 μm, 25 μm, and 67 μm APS, respectively, and are enhanced 4.7 times, 7.8 times, and 8.2 times compared to that of the plain Cu surface. A further increase of the thickness from the optimized value resulted in a sharp decrease of the maximum NBHT coefficient owing to an increase in the thermal conduction resistance of vapor in the porous layer. The maximum NBHT coefficients increase by approximately 68% as the particle size increases from 10 μm to 25 μm. However, the maximum NBHTs of 25 μm and 67 μm APS are close.

The particle size effect on the pool boiling curves are more clearly seen by comparing the optimized boiling curves of each particle size in Fig. 11. The boiling curves show that the CHF increases from 1,475 kW/m^2 to 2,025 kW/m^2 as the particle size increases from 10 μm to 67 μm (Fig. 11A). The NBHT coefficient increases as the particle size increases from 10 μm to 67 μm (Fig. 11B). The highest NBHT coefficient value of approximately 400 kW/m^{2}K was measured with APS 67 μm near the CHF. From the results, it appears that the larger particle sizes have higher NBHT coefficients and CHF values for the tested sizes.

The enhancement of the CHF observed in the microporous coatings could be the result of the combination of hydrodynamic theory and wicking caused by capillary force. Polezhaev and Kavalev [14] developed a CHF formula for a porous structure and hypothesized that the maximum vapor velocity is much higher due to the smaller vapor column size and the vapor jet spacing interval. This suggests another mechanism that could increase the CHF from porous surfaces by having higher maximum vapor velocity in conjunction with Helmholtz instability. By contrast, Tehver [15] developed a CHF formula and concluded that the CHF increases due to the capability of liquid suction by porous coatings. Based on the current experimental results of sintered microporous coatings in saturated water at 1 atm, the CHF values increase as the particle size increases and the maximum CHF values of 25 μm and 67 μm are the same, reaching about double that of a plain Cu surface, as shown in Fig. 12. It is believed that the higher CHF of the microporous coating could be predominantly attributed to the increase in maximum vapor velocity by smaller vapor jets originated from the porous layer following Polezhaev and Kavalev [14], although wetting has some influences on the CHF. More detailed and thorough study of hydrodynamic and wetting effects on the CHF of the microporous coating need to be further carried out in the future.

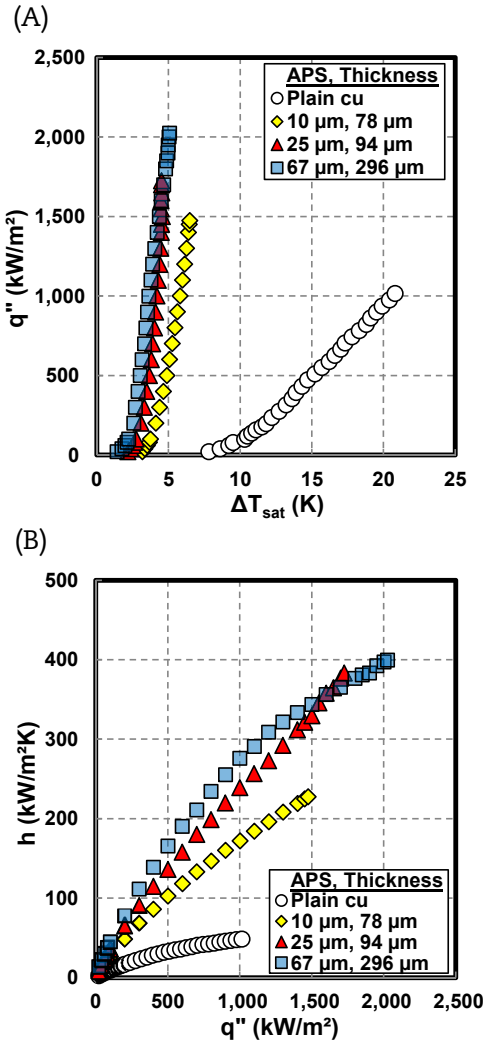

Fig. 11 – (A) Pool boiling curves and (B) Nucleate boiling heat transfer coefficients at the optimized coating thicknesses of each particle size (APS).

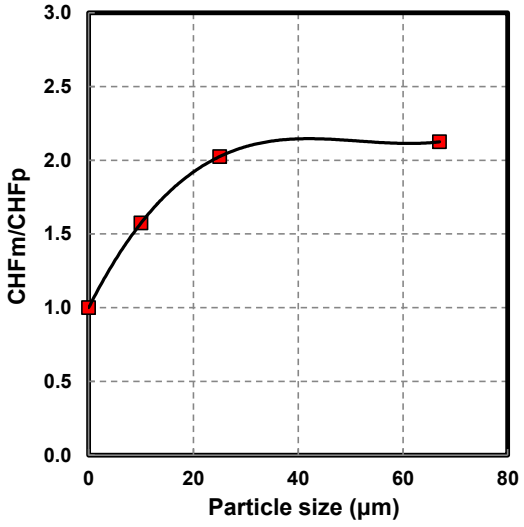

Fig. 12 – The normalized critical heat flux (CHF) at the highest CHF versus particle size.

4. Conclusions

An experiment on the pool boiling heat transfer of water saturated at atmospheric pressure was conducted to investigate the effect of Cu-sintered HTCMC on the flat Cu surface with the change in particle size and coating thickness. The optimized coating thicknesses were obtained at 78 μm, 94 μm, and 296 μm for APS 10 μm, 25 μm, and 67 μm, respectively. As the coating thickness increased further from the optimized thickness, the NBHT coefficient decreased sharply, whereas the CHF increased slightly in the tested range. As the particle size increased, both the CHF and NBHT coefficients increased. The highest CHF and NBHT coefficient were found to be approximately 2.1 MW/m^2 and approximately 400 kW/m^2K at APS 67 μm, and these values are approximately double and eight times higher than those of a plain surface.

Conflicts of interest

All authors have no conflicts of interest to declare.

Acknowledgments

This work was supported by the National Research Foundation of Korea (NRF) grant funded by the Korea government (Ministry of Science, ICT, and Future Planning; Grant No. 2012 M2A8A4025885).

REFERENCES

[1] J.P. O'Connor, S.M. You, A painting technique to enhance pool boiling heat transfer in saturated FC-72, J. Heat Transfer 117 (1995) 387–393.
[2] J.P. O'Connor, S.M. You, D.C. Price, A dielectric surface coating technique to enhance boiling heat transfer from high power microelectronics, IEEE Trans. Comp. Packag. Manufact. Technol. A 18 (1995) 656–663.
[3] J.Y. Chang, S.M. You, Heater orientation effects on pool boiling of micro-porous-enhanced surfaces in saturated FC-72, J. Heat Transfer 118 (1996) 937–943.
[4] M.B. Dizon, J. Yang, F.B. Cheung, J.L. Rempe, K.Y. Suh, S.B. Kim, Effects of surface coating on the critical heat flux for pool boiling from a downward facing surface, J. Enhanced Heat Transfer 11 (2004) 133–150.
[5] C. Li, G.P. Peterson, Geometric effects on critical heat flux on horizontal microporous coatings, J. Thermophys. Heat Transfer 24 (2010) 449–455.
[6] J.H. Kim, A. Gurung, M. Amaya, S.M. Kwark, S.M. You, Microporous coatings to maximize pool boiling heat transfer of saturated R-123 and water, J. Heat Transfer 137 (2015) 081501.
[7] S. Jun, H. Wi, A. Gurung, M. Amaya, S.M. You, Pool boiling heat transfer enhancement of water using brazed copper microporous coatings, Proc.. of 2015 ASME International Mechanical Engineering & Exposition, IMECE2015, IMECE-52044, ASME Houston, Texas, USA, 2015. accepted.
[8] S.M. Lu, R.H. Chang, Pool boiling from a surface with a porous layer, AlChE J. 33 (1987) 1813–1828.
[9] J.Y. Chang, S.M. You, Boiling heat transfer phenomena from microporous and porous surfaces in saturated FC-72, Int. J. Heat Mass Transfer 40 (18) (1997) 4437–4447.
[10] G.S. Hwang, M. Kaviany, Critical heat flux in thin, uniform particle coatings, Int. J. Heat Mass Transfer 49 (2006) 844–849.
[11] S.J. Kline, F.A. McClintock, Describing uncertainties in single-sample experiments, Mech. Eng. 75 (1953) 3–8.
[12] P. Griffith, J.D. Wallis, The role of surface conditions in nucleate boiling, The Office of Naval Research,, Technical report No. 14 (1958) 1–16.
[13] R. Webb, Nucleate boiling on porous coated surfaces, Heat Thermal Eng. 4 (1983) 71–82.
[14] Y.V. Polezhaev, S.A. Kovalev, Modeling heat transfer with boiling on porous structures, Thermal Eng. 37 (1990) 617–620.
[15] J. Tehver, Influence of porous coating on the boiling burnout heat flux, Rec. Adv. Heat Transfer (1992) 231–242.